THE GEOLOGICAL SOCIETY OF AMERICA®

Subduction initiation dynamics along a transform fault control trench curvature and ophiolite ages

Xin Zhou[1,2,3,4], Zhong-Hai Li[4]*, Taras V. Gerya[3], Robert J. Stern[5], Zhiqin Xu[6], and Jinjiang Zhang[2]
[1]Institute of Geology, Chinese Academy of Geological Sciences, Beijing 100037, China
[2]School of Earth and Space Sciences, Peking University, Beijing 100871, China
[3]Institute of Geophysics, ETH-Zürich, 8092 Zurich, Switzerland
[4]Key Laboratory of Computational Geodynamics, College of Earth and Planetary Sciences, University of Chinese Academy of Sciences, Beijing 100049, China
[5]Geosciences Department, University of Texas at Dallas, Richardson, Texas 75080, USA
[6]School of Earth Sciences and Engineering, Nanjing University, Nanjing 210023, China

ABSTRACT

Understanding how new subduction zones form is essential for complete articulation of plate tectonic theory. Formation of new subduction zones by collapse of oceanic transform faults or fracture zones is suggested on the basis of empirical evidence. This process has heretofore been investigated with two-dimensional (2-D) numerical models, which thus ignore its intrinsic three-dimensional (3-D) geometry, lateral propagation, and dynamics. Here, we investigate a 3-D thermomechanical model, in which old and thick oceanic lithosphere (plate) is separated by a transform fault from a thinner and younger oceanic plate containing a transform-orthogonal spreading ridge. The results suggest that the older plate starts to sink spontaneously at the ridge–transform fault junction, and then subduction initiation laterally propagates along the transform away from the ridge. Two key factors control the 3-D subduction initiation (SI) dynamics in nature: (1) the age of the sinking plate, which controls its negative buoyancy; and (2) the thermal structure of the overriding plate, which reflects its spreading history. Our numerical models not only shed new light on the SI dynamics of Cenozoic subduction zones (e.g., the Izu-Bonin-Mariana zone in the Pacific Ocean), but also have implications for fossil convergent plate margins (e.g., the Bitlis-Zagros suture zone, west of the Strait of Hormuz). In the latter case, systematic variations in ages of supra–subduction zone ophiolites may reflect diachronous SI and its lateral propagation.

INTRODUCTION

Subduction initiation (SI), either induced or spontaneous, occurs most readily in oceanic lithosphere. Induced SI generally leads to compressional uplift in the forearc region (Hall et al., 2003; Mao et al., 2017), whereas spontaneous SI causes extension and magmatism (Arculus et al., 2015; Stern, 2004). It is generally accepted that the negative buoyancy of sufficiently old oceanic lithosphere provides the key driving force for SI; however, the dynamic processes are still widely debated (Gerya, 2011; Gurnis et al., 2004; Stern, 2004; Stern and Gerya, 2018). For intra-oceanic subduction systems, previous studies suggest that transform faults and fracture zones are potential sites for SI (Deschamps and Lallemand, 2003; Hall et al., 2003; Uyeda and Ben-Avraham, 1972), especially where the neighboring two plates have a significant age difference, and thus large density contrast. Transform faults and fracture zones provide localized lithospheric weaknesses of great length, thus providing favorable sites and conditions for SI. Transform fault–related SI has been studied via both geological observations and numerical models. For example, the Izu-Bonin-Mariana (IBM) subduction zone (Pacific Ocean) is generally considered a good candidate for studying this SI mode, in which the composition of magmatic rocks erupted during Eocene SI evolved from forearc basaltic, boninitic, and tholeiitic to calc-alkaline (Ishizuka et al., 2011, 2014; Leng et al., 2012), representing the dynamic transition from SI to mature subduction. Another significant characteristic of convergent margins is the large concave curvature of the trench, which may result from either the SI stage or the retreating subduction stage. Understanding the along-strike variations of SI calls for three-dimensional (3-D) numerical models.

Besides young (Cenozoic) SI examples such as IBM, more ancient examples may be represented by supra–subduction zone (SSZ) ophiolites, which record magmatic activity associated with early stages of intra-oceanic subduction (Pearce, 2003). Thus, the spatial and temporal distributions of SSZ ophiolites are critical clues to understanding SI history (Stern et al., 2012). Previous studies also demonstrate that forearc ophiolites obduct along the strike of transform faults during SI (Dewey and Casey, 2011). Based on existing geochronological data, the along-strike age distribution of Late Cretaceous SSZ ophiolites in the eastern Mediterranean-Zagros orogen indicates that ophiolites in the central region are ~5–10 m.y. older than those on either side, which may reflect the start and lateral propagation of SI along a preexisting transform-fracture zone (Shafaii Moghadam et al., 2013a). These typical along-strike variations are crucial for understanding the full dynamics of SI, which requires systematic numerical studies in the 3-D regime; however, such models have not been attempted yet.

In this study, we focus on the initiation and lateral propagation of new spontaneous subduction zones along transform faults, by conducting 3-D high-resolution self-driven numerical models. Following previous two-dimensional studies of transform fault–related SI, the sinking plate is expected to be older, thicker, and denser than the overriding plate. For the young overriding plate, a mid-oceanic ridge (MOR) is implemented perpendicular to the transform fault. Thereby, the overriding lithosphere is characterized by increasing ages from the MOR to both sides. The 3-D model assumes a spreading ridge, but the SI may not require this. Generally, the inactive spreading ridge in the model may represent a certain overriding plate extension and significant along-strike heterogeneity. The initial model configuration is shown in Figure DR1 in the GSA Data Repository[1]. With such a basic model setup, systematic numerical models are conducted with variable ages of the subducting plate and different MOR-related structure of the overriding plate (symmetric versus asymmetric).

*E-mail: li.zhonghai@ucas.ac.cn

[1]GSA Data Repository item 2018208, model configuration, numerical methods, additional results and discussion, is available online at http://www.geosociety.org/datarepository/2018/ or on request from editing@geosociety.org.

Detailed numerical parameters are summarized in the Data Repository.

NUMERICAL MODEL RESULTS

In the reference model, the initial age of the subducting plate is 100 Ma. For the symmetric overriding plate with the MOR in the center, the lithospheric age varies from 0 Ma at the MOR to 20 Ma on both sides. Lithospheric collapse begins spontaneously at the ridge–transform fault junction in the center of the model (Figs. 1A and 1B), which is driven by the negative buoyancy of the old oceanic lithosphere. The age and properties of the overriding plate determine the resistance of SI. The younger, hotter, and thinner MOR is the weakest point, thus causing SI to begin next to it. After starting in the center, SI propagates laterally to both sides, driven by both the local negative buoyancy and the pull of the neighboring subducted slab (Figs. 1C and 1D).

The SI of the whole old lithosphere occurs after ca. 5.26 Ma, which indicates an average SI propagation rate of ~19 cm/yr. In the early stage, SI propagates rapidly due to the large age and density contrast between the subducting and overriding plates. A straight trench following the transform forms during this stage (Fig. 2A). When SI propagates farther away from the MOR, the propagation rates slow due to larger resistance from increasingly older and thicker overriding plate. In this stage, the subducting slab in the center sinks and retreats faster; however, the along-strike propagation is slower. Thus, the extension of the overriding plate is forced to respond, creating a wider forearc where the ridge-transform intersection was. Consequently, large concave curvature of the trench results (Figs. 2B). When the whole subducting plate (which is limited laterally by two free-slip model boundaries serving as two extremely weak subduction-transform edge propagator faults; Govers and Wortel, 2005) begins to subduct into the mantle, the concavity decreases, indicating a lessening effect of overriding plate resistance (Fig. 2C). The age of subducting oceanic lithosphere is also a critical parameter because this controls the density and thus the negative buoyancy, which further determines the trench geometry and SI propagation rates (cf. Figs. 3A–3C).

GEOLOGICAL IMPLICATIONS

The IBM subduction zone is the typical example for SI because of the well-studied sequence of magmatic rocks generated from SI to mature subduction, as revealed by the recent International Ocean Discovery Program (IODP) drilling (Arculus et al., 2015; Reagan et al., 2017). When the old and dense lithosphere collapses and sinks into the mantle, hot asthenosphere upwells and experiences decompression melting, which results in the first magmas having MOR basalt (MORB)–like compositions. Rapid trench

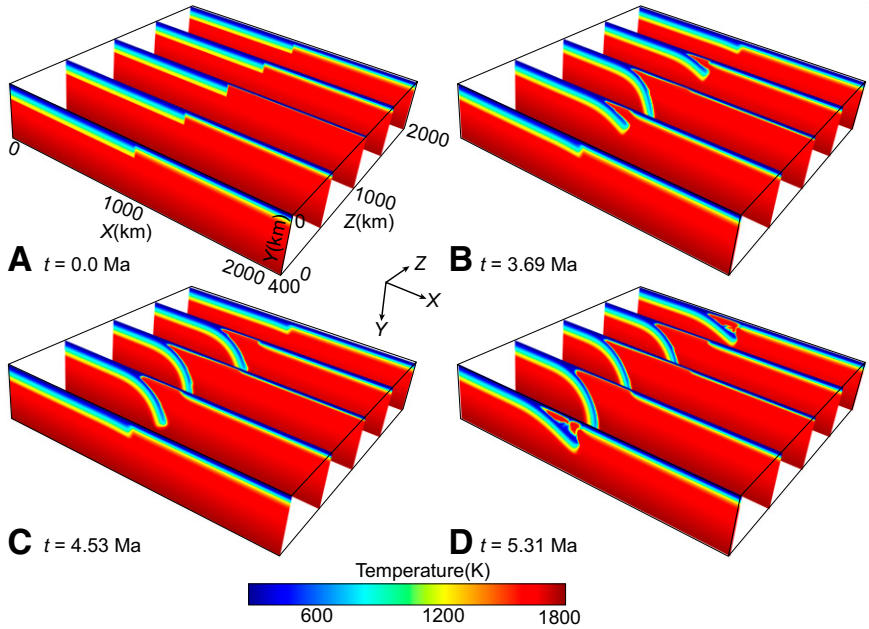

Figure 1. Modeled subduction initiation along transform fault separating old sinking plate (left side) from young overriding plate with mid-ocean ridge (right side) (*t*—time). Subduction initiation first occurs at transform fault–ridge junction in center, and then laterally propagates along transform to both sides. Animation of this sequence can be found in the Data Repository (see footnote 1).

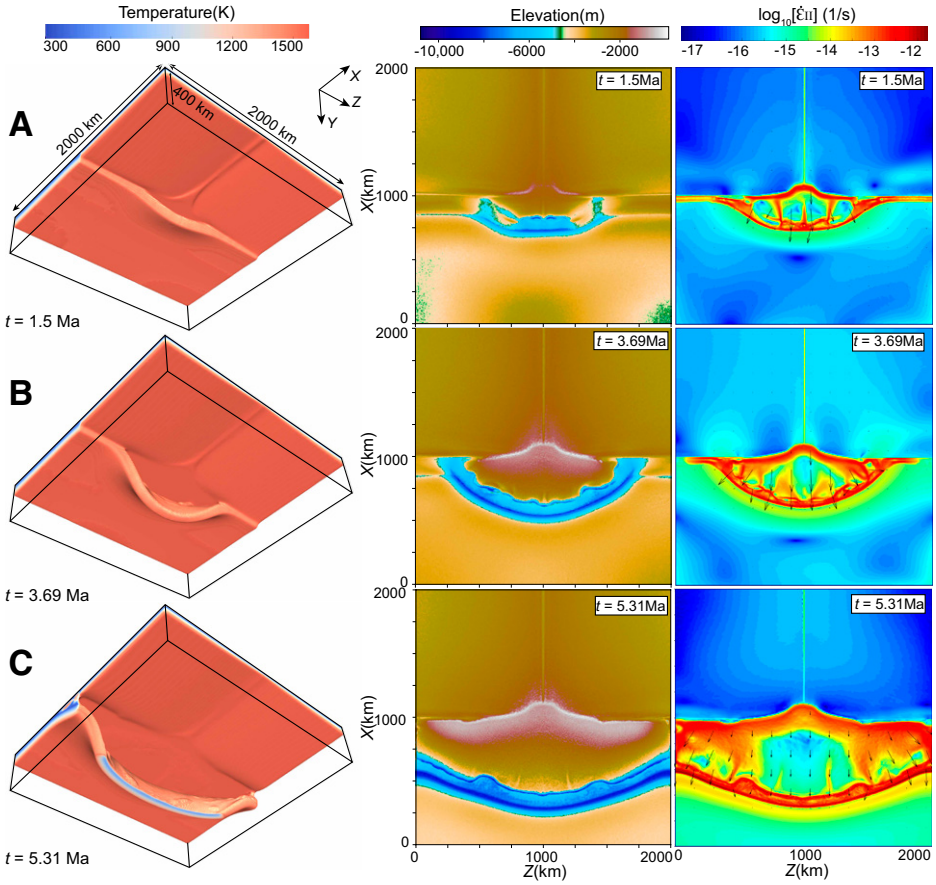

Figure 2. Schematic diagram showing development of subduction initiation propagation along transform fault. First column shows bottom view of subducting and overriding plates. Second column shows top view of topography evolution. Third column shows second invariant of strain rate at a constant depth of 25 km, in which the velocity field is represented by black arrows ($\dot{\varepsilon}_{II}$ is the second invariant of strain rate tensor). Animations can be found in the Data Repository (see footnote 1).

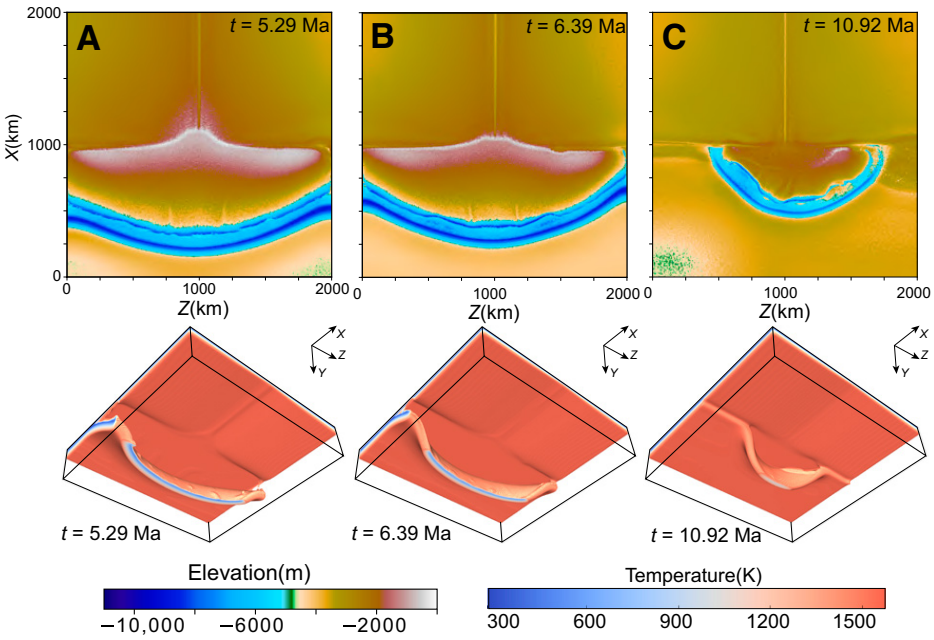

Figure 3. Models with different ages of subducting oceanic plate. A: 100 Ma. B: 70 Ma. C: 40 Ma. Overriding plates are same in each model, with ages of 0 Ma to 20 Ma from central mid-ocean ridge (MOR) to lateral edges. Top row shows top view of topography evolution. Bottom row shows bottom view of subducting and overriding plates.

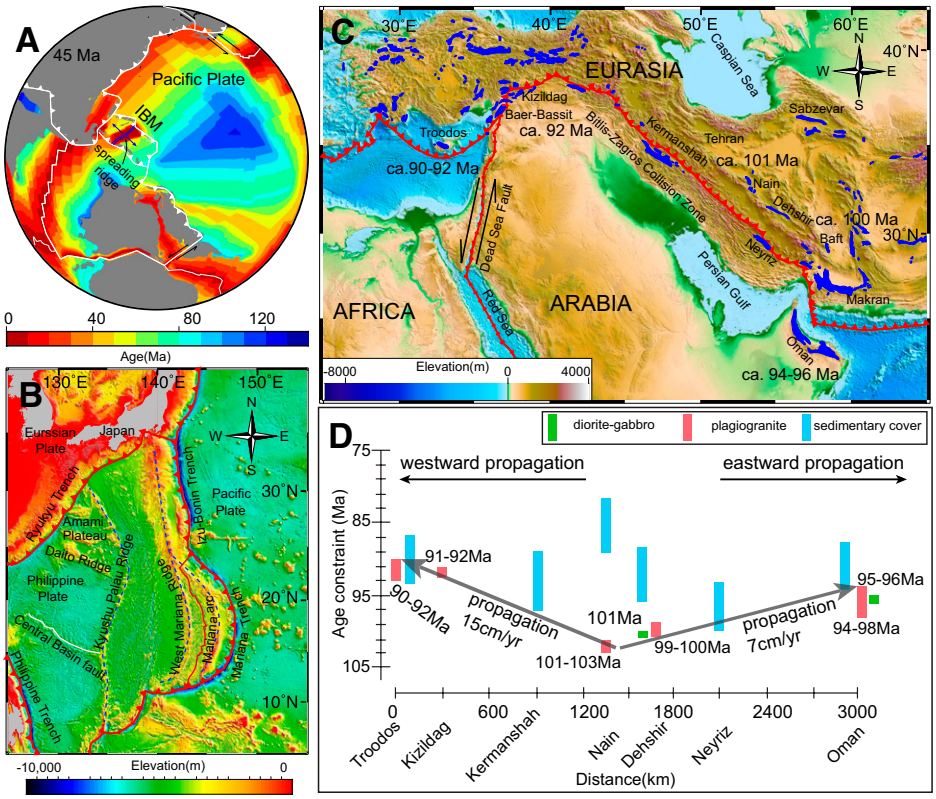

Figure 4. A: Global plate tectonic reconstruction at 45 Ma, showing that Pacific plate subducts under mid-ocean ridge along Izu-Bonin-Mariana (IBM) subduction zones (data from Müller et al., 2008). B: Modern IBM subduction zones. C: Tectonic setting of eastern Mediterranean-Zagros region and compiled ages of ophiolites (blue areas) along suture zone (data from Mann and Taira, 2004; Shafaii Moghadam et al., 2013a). D: Simplified chart showing regular age distribution of supra–subduction zone (SSZ) ophiolites along Bitlis-Zagros suture zone (after Shafaii Moghadam et al., 2013a), which implies that subduction initiation propagated along strike, consistent with our numerical models. The x-axis represents the geographic locations of the ophiolites.

retreat during the initial subduction adjacent to the overriding MOR is clearly demonstrated in our numerical models. Plate tectonic reconstructions have shown that the IBM subduction zones originated from collapse of the Pacific plate adjacent to a transform fault with a MOR on the overriding plate (Fig. 4A) (Casey and Dewey, 1984; Deschamps and Lallemand, 2003), which is consistent with our numerical models.

The SI process along the strike of the trench is still unclear in the IBM subduction zone. Our numerical models provide an optional evolution model, which is related to the along-strike diachronism of SI. IBM SI strongly depends on the MOR configuration of the overriding plate. It has long been known that the Central Basin fault in the West Philippine Sea marks the location of a Paleogene spreading ridge (Fig. 4A; Fujioka et al., 1999), although most of its spreading happened after SI. Consequently, it would have been easiest for subduction to have initiated in this region, due to the extremely young overriding plate and thus low resistance. Afterward, SI would have propagated to both the north and south and may have formed a curved trench. The Kyushu Palau Ridge is thought to approximate the residual trace of the original IBM trench (Ishizuka et al., 2018). Because this ridge (Fig. 4B) does not show strong curvature, IBM SI may have experienced very fast along-strike propagation, which is consistent with the existing age constraints (Ishizuka et al., 2018). Previous studies indicate the subducting plate was ca. 50–70 Ma in age during IBM SI (Hall et al., 2003; Leng and Gurnis, 2015), which may have resulted in fast propagation rates and thus less curvature. This is consistent with what we see today for the trace of the Kyushu Palau Ridge. The evolution of the ridge and its relation to the original locus of IBM SI requires further study to test our model.

Three-dimensional numerical modeling of spontaneous SI along a transform fault is useful not only for understanding recent subduction zones (e.g., IBM), but also for understanding older ones that have evolved into collisional orogens. SSZ ophiolites represent oceanic lithosphere that formed in the upper plate during SI, analogous to the forearcs of modern intra-oceanic convergent margins (Ishizuka et al., 2014; Stern, 2010; Stern et al., 2012), such as IBM. Late Cretaceous ophiolites along the Bitlis-Zagros suture zone in Cyprus, Turkey, Syria, Iran, and Oman have clear SSZ geochemical affinities and are increasingly interpreted to represent Neotethyan forearc oceanic lithosphere (Shafaii Moghadam et al., 2013a, 2013b). A recent compilation of geochronological data indicates that the Nain and Dehshir ophiolites in the middle of this belt formed at ca. 100 Ma, and the ages of Zagros ophiolites are younger on both sides (see Fig. 4C). These age relationships indicate that Late Cretaceous SI may have

begun in the center (Zagros) and then laterally propagated to both the west and east. From the central to the western part of the belt, the inferred propagation rate was ~15 cm/yr, while SI propagated at ~7 cm/yr from the central to the eastern part (Fig. 4D) (Shafaii Moghadam et al., 2013b).

According to the numerical models, the propagation of SI along the transform faults or fracture zones highly depends on the overriding plate. The heterogeneity of the overriding plate may be the controlling factor, which led to the diachronous distribution of SSZ ophiolites along the Bitlis-Zagros orogen. The SSZ ophiolites formed essentially *in situ* along a pre–Late Cretaceous transform fault near the continental edge and were then deformed during subsequent subduction and continental collision. The propagation rates in our numerical models with old subducting plate (e.g., 100 Ma) are a bit faster (~19 cm/yr) than those determined from the geological data (7–15 cm/yr). In addition, the younger sinking slab and/or older overriding plate would have led to slower along-strike propagation of SI (Table DR3 in the Data Repository). The diachronous tectonic evolution explains how a new subduction zone may have begun in the Late Cretaceous on the southwest margin of Eurasia and propagated along this margin.

CONCLUSION

We use 3-D thermo-mechanical numerical models to investigate spontaneous SI and its lateral propagation along a transform fault. The main conclusions we draw from this study are:

(1) SI along a transform fault is expected to be a diachronous process in which SI is likely to begin at the weakest point—the ridge–transform fault junction—and then propagate laterally.

(2) In the early stage, SI propagates rapidly due to the large age and density contrast between the subducting and overriding plates. A straight trench forms during this stage. In the later stage, the SI propagation rates slow and large concave curvature of the arc-trench system develops.

(3) Along-strike propagation rates of SI depend on the age contrast between the subducting plate and the overriding plate and are likely to vary from 5 to 20 cm/yr.

(4) The modern Izu-Bonin-Mariana convergent margin may have formed as a result of collapse of the Pacific plate along a transform fault, with SI starting at the transform-ridge junction and then propagating along the transform in both directions.

(5) The distribution of SSZ ophiolites with different ages along orogenic belts (e.g., Bitlis-Zagros suture zone) may represent the start and lateral propagation of SI.

ACKNOWLEDGMENTS

This work was supported by the Strategic Priority Research Program (B) of the Chinese Academy of Sciences (XDB18000000), China Natural Science Foundation projects (41622404, 41774108, 41688103), as well as the China Scholarship Council. Gerya acknowledges support from European Union projects CREEP and SUBITOP. This is University of Texas at Dallas Geosciences contribution number 1325. Thorough and constructive reviews by M. Gurnis, J. Dewey, P. Ryan, and the editor D. Brown are much appreciated.

REFERENCES CITED

Arculus, R.J., et al., 2015, A record of spontaneous subduction initiation in the Izu-Bonin-Mariana arc: Nature Geoscience, v. 8, p. 728–733, https://doi.org/10.1038/ngeo2515.

Casey, J.F., and Dewey, J.F., 1984, Initiation of subduction zones along transform and accreting plate boundaries, triple-junction evolution, and forearc spreading centres—Implications for ophiolitic geology and obduction, *in* Gass, I.G., et al., eds., Ophiolites and Oceanic Lithosphere: Geological Society of London Special Publication 13, p. 269–290, https://doi.org/10.1144/GSL.SP.1984.013.01.22.

Deschamps, A., and Lallemand, S., 2003, Geodynamic setting of Izu-Bonin-Mariana boninites, *in* Larter, R.D., and Leat, P.T., eds., Intra-Oceanic Subduction Systems: Tectonic and Magmatic Processes: Geological Society of London Special Publication 219, p. 163–185, https://doi.org/10.1144/GSL.SP.2003.219.01.08.

Dewey, J.F., and Casey, J.F., 2011, The origin of obducted large-slab ophiolite complexes, *in* Brown, D., and Ryan, P.D., eds., Arc-Continent Collision: Berlin Heidelberg, Springer Verlag, Frontiers in Earth Sciences, v. 4, p. 431–444, https://doi.org/10.1007/978-3-540-88558-0_15.

Fujioka, K., Okino, K., Kanamatsu, T., Ohara, Y., Ishizuka, O., Haraguchi, S., and Ishii, T., 1999, Enigmatic extinct spreading center in the West Philippine backarc basin unveiled: Geology, v. 27, p. 1135–1138, https://doi.org/10.1130/0091-7613(1999)027<1135:EESCIT>2.3.CO;2.

Gerya, T., 2011, Future directions in subduction modeling: Journal of Geodynamics, v. 52, p. 344–378, https://doi.org/10.1016/j.jog.2011.06.005.

Govers, R., and Wortel, M.J.R., 2005, Lithosphere tearing at STEP faults: Response to edges of subduction zones: Earth and Planetary Science Letters, v. 236, p. 505–523, https://doi.org/10.1016/j.epsl.2005.03.022.

Gurnis, M., Hall, C., and Lavier, L., 2004, Evolving force balance during incipient subduction: Geochemistry Geophysics Geosystems, v. 5, Q07001, https://doi.org/10.1029/2003GC000681.

Hall, C.E., Gurnis, M., Sdrolias, M., Lavier, L.L., and Müller, R.D., 2003, Catastrophic initiation of subduction following forced convergence across fracture zones: Earth and Planetary Science Letters, v. 212, p. 15–30, https://doi.org/10.1016/S0012-821X(03)00242-5.

Ishizuka, O., Tani, K., Reagan, M.K., Kanayama, K., Umino, S., Harigane, Y., Sakamoto, I., Miyajima, Y., Yuasa, M., and Dunkley, D.J., 2011, The timescales of subduction initiation and subsequent evolution of an oceanic island arc: Earth and Planetary Science Letters, v. 306, p. 229–240, https://doi.org/10.1016/j.epsl.2011.04.006.

Ishizuka, O., Tani, K., and Reagan, M.K., 2014, Izu-Bonin-Mariana forearc crust as a modern ophiolite analogue: Elements, v. 10, p. 115–120, https://doi.org/10.2113/gselements.10.2.115.

Ishizuka, O., Hickey-Vargas, R., Arculus, R.J., Yogodzinski, G.M., Savov, I.P., Kusano, Y., Mccarthy, A., Brandl, P.A., and Sudo, M., 2018, Age of Izu-Bonin-Mariana arc basement: Earth and Planetary Science Letters, v. 481, p. 80–90, https://doi.org/10.1016/j.epsl.2017.10.023.

Leng, W., and Gurnis, M., 2015, Subduction initiation at relic arcs: Geophysical Research Letters, v. 42, p. 7014–7021, https://doi.org/10.1002/2015GL064985.

Leng, W., Gurnis, M., and Asimow, P., 2012, From basalts to boninites: The geodynamics of volcanic expression during induced subduction initiation: Lithosphere, v. 4, p. 511–523, https://doi.org/10.1130/L215.1.

Mann, P., and Taira, A., 2004, Global tectonic significance of the Solomon Islands and Ontong Java Plateau convergent zone: Tectonophysics, v. 389, p. 137–190, https://doi.org/10.1016/j.tecto.2003.10.024.

Mao, X., Gurnis, M., and May, D.A., 2017, Subduction initiation with vertical lithospheric heterogeneities and new fault formation: Geophysical Research Letters, v. 44, p. 11,349–11,356, https://doi.org/10.1002/2017GL075389.

Müller, R.D., Sdrolias, M., Gaina, C., and Roest, W.R., 2008, Age, spreading rates, and spreading asymmetry of the world's ocean crust: Geochemistry Geophysics Geosystems, v. 9, Q04006, https://doi.org/10.1029/2007GC001743.

Pearce, J.A., 2003, Supra-subduction zone ophiolites: The search for modern analogues, *in* Dilek, Y., and Newcomb, S., eds., Ophiolite Concept and the Evolution of Geological Thought: Geological Society of America Special Paper 373, p. 269–293, https://doi.org/10.1130/0-8137-2373-6.269.

Reagan, M.K., et al., 2017, Subduction initiation and ophiolite crust: New insights from IODP drilling: International Geology Review, v. 59, p. 1439–1450, https://doi.org/10.1080/00206814.2016.1276482.

Shafaii Moghadam, H., Corfu, F., and Stern, R.J., 2013a, U-Pb zircon ages of Late Cretaceous Nain-Dehshir ophiolites, central Iran: Journal of the Geological Society, v. 170, p. 175–184, https://doi.org/10.1144/jgs2012-066.

Shafaii Moghadam, H., Stern, R.J., Chiaradia, M., and Rahgoshay, M., 2013b, Geochemistry and tectonic evolution of the Late Cretaceous Gogher-Baft ophiolite, central Iran: Lithos, v. 168–169, p. 33–47, https://doi.org/10.1016/j.lithos.2013.01.013.

Stern, R.J., 2004, Subduction initiation: Spontaneous and induced: Earth and Planetary Science Letters, v. 226, p. 275–292, https://doi.org/10.1016/S0012-821X(04)00498-4.

Stern, R.J., and Gerya, T., 2018, Subduction initiation in nature and models: A review: Tectonophysics, https://doi.org/10.1016/j.tecto.2017.10.014 (in press).

Stern, R.J., Reagan, M., Ishizuka, O., Ohara, Y., and Whattam, S., 2012, To understand subduction initiation, study forearc crust: To understand forearc crust, study ophiolites: Lithosphere, v. 4, p. 469–483, https://doi.org/10.1130/L183.1.

Uyeda, S., and Ben-Avraham, Z., 1972, Origin and development of the Philippine Sea: Nature Physical Science, v. 240, p. 176–178, https://doi.org/10.1038/physci240176a0.

Manuscript received 8 February 2018
Revised manuscript received 15 May 2018
Manuscript accepted 17 May 2018

Printed in USA